






# The *Parauncinula polyspora* Draft Genome Provides Insights into Patterns of Gene Erosion and Genome Expansion in Powdery Mildew Fungi

Lamprinos Frantzeskakis,<sup>a,\*</sup> Márk Z. Németh,<sup>b</sup> Mirna Barsoum,<sup>a</sup>  Stefan Kusch,<sup>a</sup>  Levente Kiss,<sup>c</sup> Susumu Takamatsu,<sup>c,d</sup>  Ralph Panstruga<sup>a</sup>

<sup>a</sup>Institute for Biology I, Unit of Plant Molecular Cell Biology, RWTH Aachen University, Aachen, Germany

<sup>b</sup>Plant Protection Institute, Centre for Agricultural Research, Hungarian Academy of Sciences, Budapest, Hungary

<sup>c</sup>Centre for Crop Health, University of Southern Queensland, Toowoomba, Australia

<sup>d</sup>Faculty of Bioresources, Mie University, Tsu, Japan

**ABSTRACT** Due to their comparatively small genome size and short generation time, fungi are exquisite model systems to study eukaryotic genome evolution. Powdery mildew fungi present an exceptional case because of their strict host dependency (termed obligate biotrophy) and the atypical size of their genomes (>100 Mb). This size expansion is largely due to the pervasiveness of transposable elements on 70% of the genome and is associated with the loss of multiple conserved ascomycete genes required for a free-living lifestyle. To date, little is known about the mechanisms that drove these changes, and information on ancestral powdery mildew genomes is lacking. We report genome analysis of the early-diverged and exclusively sexually reproducing powdery mildew fungus *Parauncinula polyspora*, which we performed on the basis of a natural leaf epiphytic metapopulation sample. In contrast to other sequenced species of this taxonomic group, the assembled *P. polyspora* draft genome is surprisingly small (<30 Mb), has a higher content of conserved ascomycete genes, and is sparsely equipped with transposons (<10%), despite the conserved absence of a common defense mechanism involved in constraining repetitive elements. We speculate that transposable element spread might have been limited by this pathogen's unique reproduction strategy and host features and further hypothesize that the loss of conserved ascomycete genes may promote the evolutionary isolation and host niche specialization of powdery mildew fungi. Limitations associated with this evolutionary trajectory might have been in part counteracted by the evolution of plastic, transposon-rich genomes and/or the expansion of gene families encoding secreted virulence proteins.

**IMPORTANCE** Powdery mildew fungi are widespread and agronomically relevant phytopathogens causing major yield losses. Their genomes have disproportionately large numbers of mobile genetic elements, and they have experienced a significant loss of highly conserved fungal genes. In order to learn more about the evolutionary history of this fungal group, we explored the genome of an Asian oak tree pathogen, *Parauncinula polyspora*, a species that diverged early during evolution from the remaining powdery mildew fungi. We found that the *P. polyspora* draft genome is comparatively compact, has a low number of protein-coding genes, and, despite the absence of a dedicated genome defense system, lacks the massive proliferation of repetitive sequences. Based on these findings, we infer an evolutionary trajectory that shaped the genomes of powdery mildew fungi.

**KEYWORDS** genome evolution, plant pathogen, fungal genomics, transposable elements, repeat-induced point mutation

**Citation** Frantzeskakis L, Németh MZ, Barsoum M, Kusch S, Kiss L, Takamatsu S, Panstruga R. 2019. The *Parauncinula polyspora* draft genome provides insights into patterns of gene erosion and genome expansion in powdery mildew fungi. *mBio* 10:e01692-19. <https://doi.org/10.1128/mBio.01692-19>.

**Editor** B. Gillian Turgeon, Cornell University

**Copyright** © 2019 Frantzeskakis et al. This is an open-access article distributed under the terms of the [Creative Commons Attribution 4.0 International license](https://creativecommons.org/licenses/by/4.0/).

Address correspondence to Ralph Panstruga, [panstruga@bio1.rwth-aachen.de](mailto:panstruga@bio1.rwth-aachen.de).

\* Present address: Lamprinos Frantzeskakis, DOE Joint Genome Institute, Walnut Creek, California, USA.

**Received** 2 July 2019

**Accepted** 20 August 2019

**Published** 24 September 2019

Due to their ubiquitous presence in diverse environments with different intensities of selection pressure, fungi provide a unique insight into the evolution of eukaryotic genomes (1). The genomes of phytopathogenic fungi in particular have been in the spotlight because of their peculiar genome architectures (2), which foster mechanisms that allow for the rapid adaptation to an ever-changing plethora of host resistance genes (3). This high genome flexibility is considered to be a valuable feature for immune evasion, virulence, and long-term survival (4).

Powdery mildews (PMs) (Ascomycota, Erysiphales) are a monophyletic group of phytopathogens (5) that exclusively colonize living host plants—a lifestyle termed obligate biotrophy (6). Species of this family can have a broad or narrow range of hosts (7, 8), some of which include important agricultural and horticultural crops (9). Typically, PMs propagate via short (several days long) asexual life cycles and the production of conidiospores, but can undergo sexual propagation by the formation of ascospores under particular circumstances (e.g., for overwintering [10]).

PMs hold a special spot in filamentous plant pathogen genomics owing to the large size of their genomes, the vast amount of transposable elements (TEs) therein, and the large-scale loss of conserved fungal genes and associated cellular pathways (11–14). Recently, different laboratories have successfully managed to tackle technical challenges associated with the advanced genomic analysis of these pathogens: e.g., bottlenecks in extracting high-molecular-weight DNA (15) or in assembling complex repetitive genomes to the chromosome (arm) level (12, 16). Based on these methodological improvements, new information was provided on the population structure (13, 17), genome architecture (12, 13, 16, 18, 19), and evolution (20) of some of the species and their specialized forms (*formae speciales* [ff. spp.]). These studies suggest that TEs in PM genomes might be associated with the rapid turnover of virulence genes (encoding effectors) in the form of copy number variation (12, 16, 21). Additionally, it has been reported that PMs have a unique genomic architecture in which TEs and genes are intertwined, while other typical attributes found in TE-inflated genomes are missing: e.g., AT-rich isochores or large-scale compartmentalization (12, 16). Since *Blumeria graminis* has appeared relatively recently in the evolutionary history of PMs (20), the above-mentioned genome characteristics are likely to represent a contemporary step in their evolution. In order to understand how the genomes of these pathogens evolved and what acted as a substrate for their unique genome architecture, it would be necessary to seek information in the genomes of early-diverged PM species.

Here we present the draft genome of the PM species *Parauncinula polyspora*, a pathogen of the East Asian oak tree *Quercus serrata*. It has been estimated that species of the genus *Parauncinula*, which form a phylogenetic sister group to all other PMs (22), diverged from other genera of the Erysiphales 80 to 90 million years ago, rendering it one of the earliest-diverged PM genera known to date (22, 23). The four known species of *Parauncinula* (*P. curvispora*, *P. polyspora*, *P. septata*, and *P. uncinata*) differ from other PMs in their unique morphology and host range and also by lacking an asexual morph (i.e., conidiospores and conidiophores) (24). Our analysis, which is based on a natural leaf epiphytic metapopulation sample, reveals that *P. polyspora* has a surprisingly compact genome with a substantially smaller number of TEs than the more recently evolved PMs, a feature that cannot be attributed to the presence of conserved ascomycete genome defense mechanisms such as repeat-induced point (RIP) mutations. In addition, we report that the *P. polyspora* genome harbors a considerable number of conserved ascomycete genes (CAGs) that were subsequently lost in other PM lineages. Taken together, the presented analysis of the *P. polyspora* genome gives unexpected insights into the evolutionary history of PM fungi and provides broad suggestions on how TE inflation can affect the genomes of fungal phytopathogens.

## RESULTS

### Assembly of the *P. polyspora* genome from metagenomic *Q. serrata* samples.

*Parauncinula polyspora* is believed to be an obligate biotroph that relies on living plant tissues for growth and reproduction (22), and *in vitro* cultures of the species on artificial

media have never been reported. Therefore, we resorted to sampling infected *Q. serrata* leaves harboring largely *P. polyspora* hyphae and ascomata (fruiting bodies) and sequenced the respective epiphytic metagenome. In order to avoid overcontamination, which could arise from sampling the entirety of the plant tissue, samples were prepared using cellulose acetate peelings (25) of the leaf epiphytic microbiota, and the respective genomic DNA was subjected to short-read sequencing. As expected, the initial data set contained sequences of a number of eukaryotic and prokaryotic taxonomic groups (see Fig. S1A in the supplemental material). Subsequently we assembled the respective short reads and followed a pipeline for stringent filtering to exclude both contaminating bacterial and eukaryotic sequences, assuming these are significantly less abundant than authentic *P. polyspora* sequences (see Fig. S1B [methods]). After filtering for bacterial sequences, two major populations of scaffolds could be separated based on k-mer depth only. One of the two, with approximately 30× coverage for each of its 1,321 scaffolds, contained sequences with similarity to PM fungi (average identity of 60% [Fig. S1C]), while the other (mostly with <5× coverage) contained a mixture of additional fungal and plant sequences. Among the filtered contigs of the first population, we identified a scaffold of extremely deep coverage (2,384×) that is identical to the deposited nucleotide sequence of the internal transcribed spacer (ITS) region for the *P. polyspora* specimen voucher MUMH4928 (see Fig. S2). DNA of this specimen was also sampled from PM-infected *Q. serrata* in the past (24).

We then annotated these scaffolds using a previously developed pipeline for the barley PM fungus (12) and split them into 495 high- and 826 low-confidence scaffolds based on the relative frequency of leotiomycete-related annotations along each sequence (Fig. S1B [methods]). In the low-confidence group, 107 scaffolds, encompassing 10.9 Mb of sequence, always contained at least one gene with homology to Leotiomycetes and one or more with homology to extraneous species in the same scaffold, probably due to chimeric misassemblies. The remaining 719 low-confidence scaffolds (20.9 Mb of total sequence) contained either genes without any leotiomycete homology (18.4% of the scaffolds [19.0 Mb of sequence]) or no hits to the nonredundant (nr) database (81.5% of scaffolds [1.9 Mb of sequence]).

The resulting 495 high-confidence scaffolds contained 6,046 genes in 28.01 Mb of sequence. The read depth over 1-kb windows of these contigs is normally distributed and is on average 231× (Fig. S1D). Out of the annotated genes in these contigs, ~97% have a detectable homolog in the Leotiomycetes (see Table S1A in the supplemental material). In terms of genome completeness, assayed using BUSCO (26), this assembly covers 90.75% of the common fungal gene space. Notably, the ratio of single-copy to duplicated BUSCO genes resembles that of other PM genome assemblies (Table S1B), indicating that our combined filtering method based on k-mer depth and sequence similarity has likely efficiently removed contaminating fungal sequences as well. Altogether, the careful epiphytic sampling method used here provided an enriched sample of *P. polyspora* sequences, while the availability of closely related PM genomes allowed the sifting of the scaffolds based on the homology of their annotations to PM genes. For the downstream analysis, we therefore used only the 495 high-confidence scaffolds and the predicted annotations they contained, knowing, however, that the rejected low-confidence scaffolds might also contain *P. polyspora*-related sequences (see above). Yet, the total amount of these (rejected) sequences is expected to represent only a small fraction of the genome according to the aforementioned BUSCO results, which are typically ~97% for PM genome assemblies (12, 18).

To validate further the correct placement of this species as an early-diverged PM but also to corroborate the PM-related content of the high-confidence contigs, we proceeded with generating a multilocus phylogeny based on 1,964 single-copy orthologs of 16 sequenced Leotiomycetes (Fig. 1A). The placement of the species by this approach at the base of the PM clade is in accordance with previous results based on ribosomal DNA (rDNA) sequences (22).

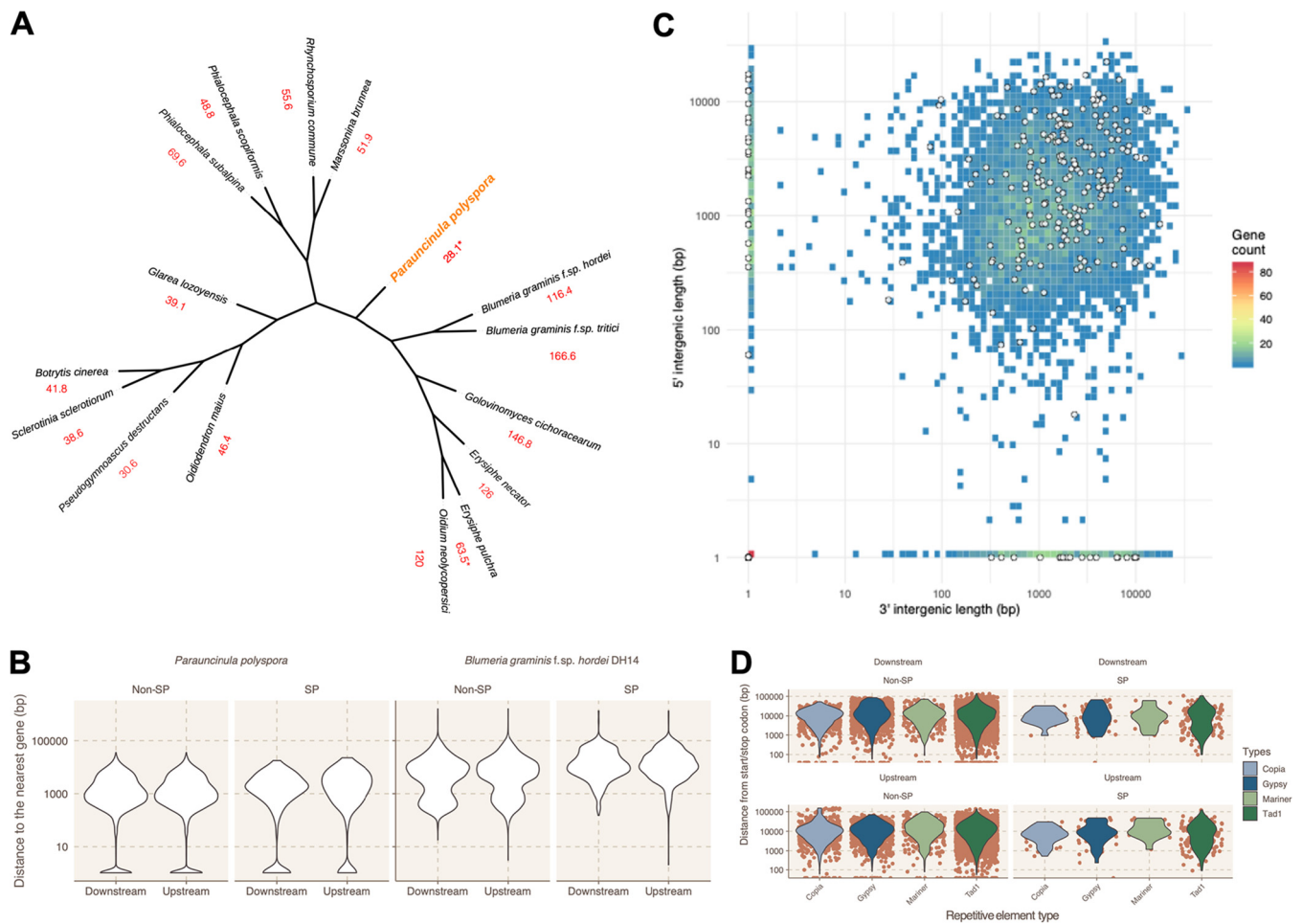


**FIG 1** Characteristics of the *P. polyspora* draft genome. (A) The multilocus phylogeny (cladogram) of selected leotiomycete fungi, based on 1,964 single-copy orthologs identified by Orthofinder, was rendered by FastTree (ML Model: Jones-Taylor-Thornton) after alignment of the sequences with MAFFT. Bootstrap support is 100% for each node. Genome sizes are given below each species in Mb (in red). Draft PM short-read assemblies where an estimate of the total genome size is not known from the literature or otherwise are marked with an asterisk at the indicated genome size. (B) Violin plots illustrating the upstream (5') and downstream (3') intergenic length (y axis [bp]) of the *P. polyspora* SP- and non-SP-coding genes in comparison to the respective intergenic distances in *B. graminis* f. sp. *hordei*. (C) Gene density plot in relation to the 5' (y axis) and 3' (x axis) intergenic distances (bp) for *P. polyspora*. White circles depict SP-coding genes. The number of genes for a given intergenic length is color coded according to the legend on the right. (D) Violin plots illustrating the distance (y axis [bp]) of TEs from the transcriptional start/stop site of SP- and non-SP-coding genes. Orange dots indicate individual data points. The type of TEs is color coded according to the legend on the right.

**The compact *P. polyspora* genome lacks large-scale compartmentalization.** The assembled *P. polyspora* draft genome is very compact (~28 Mb) compared to other sequenced PM species (Table 1), with a surprisingly small number of repetitive elements (~8.5% [Table S1C]). In order to validate this observation, we used a k-mer-based approach (27) to calculate the genome size, which returned a similar estimate of 29.1 Mb. The difference in genome size from other sequenced PMs is also reflected by the length of the intergenic space, which is on average ~3 to 4× smaller than that, e.g., in the case of *B. graminis* f. sp. *hordei* (Fig. 1B).

We noted that secreted protein-coding genes (SP genes) do not constitute a separate compartment in the *P. polyspora* draft genome: i.e., there are no extended gene-rich/gene-sparse regions with an overrepresentation of SP genes (Fig. 1C; see Fig. S3 in the supplemental material). Moreover, the comparatively few transposable elements (TEs), which nevertheless comprise representatives of all major groups (retrotransposons, long terminal repeat [LTR] elements, and DNA transposons [Table S1C]), do not exhibit preferential insertion in the proximity of SP genes (<1 kb [Fig. 1D]). Finally, we also found that contrary to *B. graminis* f. sp. *hordei*, the *P. polyspora* draft genome has a lower ratio of duplicated genes coding for SPs and non-SPs (Table S1D).

**TABLE 1** *Parauncinula polyspora* draft genome assembly and annotation statistics compared to monocot (*B. graminis* f. sp. *hordei*)- and dicot (*E. necator*)-infecting PM species

Parameter	Result for:		
	<i>P. polyspora</i>	<i>B. graminis</i> f. sp. <i>hordei</i> <sup>a</sup>	<i>E. necator</i> <sup>b</sup>
Genome assembly			
Scaffolds, no.	495	99	5,935
Size, bp			
Min	966	16,042	498
1st quartile	17,297	52,946	1,297
Median	36,067	358,063	3,420
Mean	56,598	1,176,524	8,846
3rd quartile	74,488	1,602,884	11,116
Max	354,858	9,429,963	188,576
Total	28,016,241	116,475,897	52,505,057
N value, bp			
<i>N</i> <sub>50</sub>	98,897	3,906,310	21,433
<i>N</i> <sub>90</sub>	25,733	832,904	3,975
<i>N</i> <sub>95</sub>	17,861	443,704	2,006
Total repetitive content, %	8.5	74	63
Annotation			
Genes, no.	6,046	7,118	6,484
Avg size, bp	1,548	1,423	1,419
SPs, no.	261	805	607

<sup>a</sup>See reference 12.<sup>b</sup>See reference 19.

**The *P. polyspora* mating locus is indicative of homothallism.** Typically, PM fungi, like other Pezizomycotina, have one mating-type locus with two idiomorphs called *MAT1-1* and *MAT1-2* (28). The *MAT1-1* idiomorph encodes an  $\alpha$ -domain protein and a high-mobility group (HMG) domain protein called *MAT1-1-1* and *MAT1-1-3*, respectively. The *MAT1-2* idiomorph encodes only one HMG domain protein called *MAT1-2-1* (12). Heterothallic PM fungi harbor either idiomorph in their genomes, while in rare instances of homothallism, *MAT1-2-1* and *MAT1-1-1* are present in the same genome (29). In our search of the *P. polyspora* draft genome, we identified only a single scaffold harboring mating-type genes (see Fig. S4A in the supplemental material), suggesting *P. polyspora* is a homothallic (self-fertile) PM species. These genes comprised a seemingly intact copy of *MAT1-2-1* and a likely pseudogenized copy of *MAT1-1-3* (Fig. S4B) residing ca. 10 kb away from each other on the same contig. We failed to identify a copy of *MAT1-1-1*, which is usually present in Leotiomycetes/PMs and in close physical proximity to *MAT1-1-3* (12, 30). Leotiomycete-homologous sequences representing this gene not only were lacking in the 495 high-confidence contigs but also were absent in the low-confidence contigs and the contigs with lower coverage assumed to represent contaminations. Additionally, the gene *SLA2*, which is typically found near the *MAT1* locus in many ascomycetes (30), resides on a separate scaffold, flanked by genes that are nonsyntenic to the canonical PM *MAT1* locus (Fig. S4A).

We also investigated the presence of single nucleotide polymorphisms (SNPs) and found that the majority of them are biallelic (98.2% [Table S1E]). Considering the likely homothallic nature of the species and taking into account that all PM genomes so far have been reported to be haploid during their vegetative growth phase, this finding indicates that our natural sample likely contained more than one *P. polyspora* isolate.

**The *P. polyspora* genome lacks evidence for the presence of RIP.** We proceeded in examining whether the compactness of the *P. polyspora* draft genome is due to the presence of the genome defense mechanism of RIP (31), which limits the spread of TEs and is absent in *B. graminis* f. sp. *hordei* and other sequenced PM species (6, 18, 19). We were unable to detect homologs of *Masc1*, *Masc2*, *Rid-1*, or *Dim-2* (GenBank accession no. [AAC49849.1](#), [AAC03766.1](#), [XP\\_011392925.1](#), and [XP\\_959891.1](#), respectively), which have been found to be associated with premeiotically induced DNA methylation in

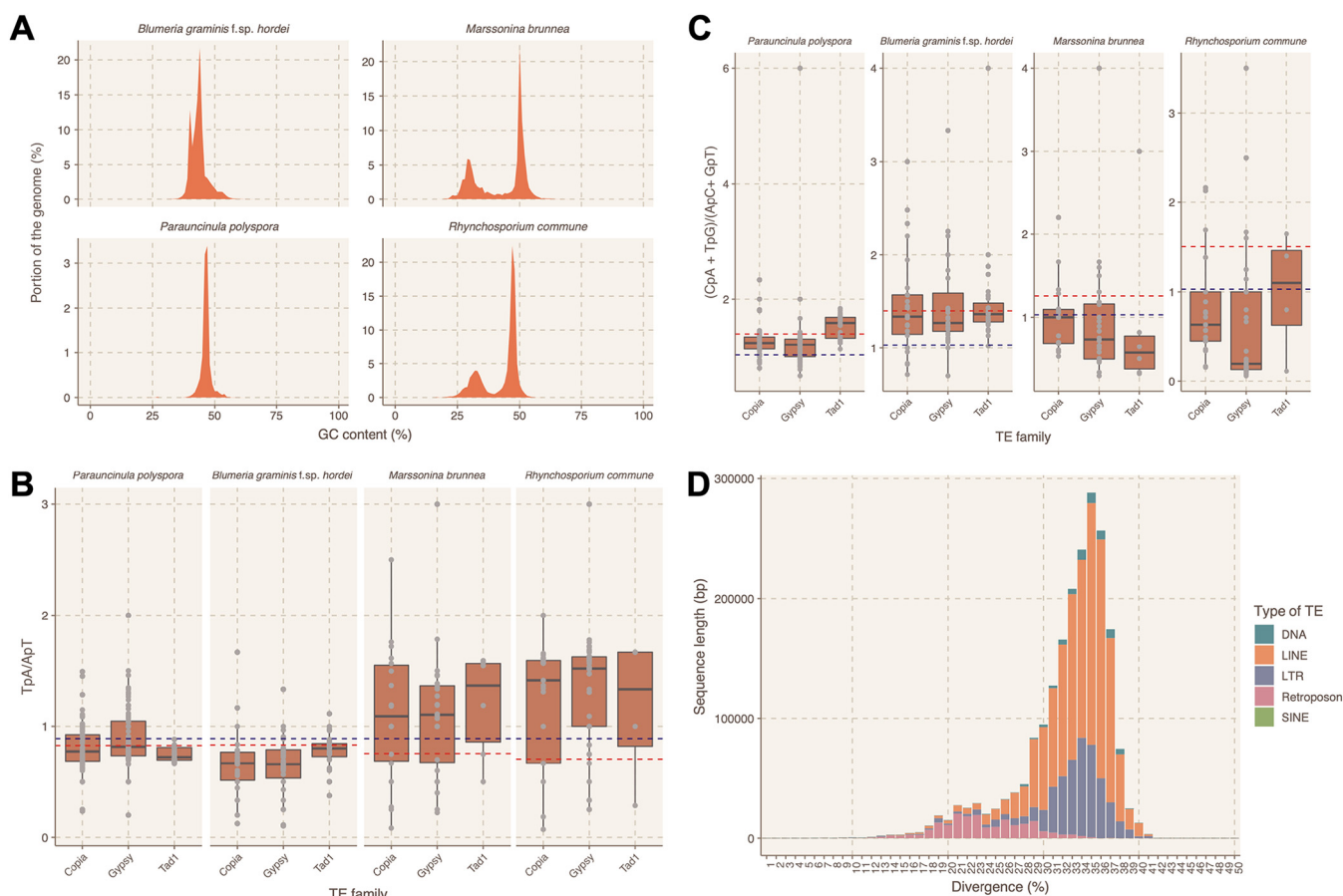


**FIG 2** Analysis for signatures of RIP in the genomes of *P. polyspora* and related Leotiomyces. (A) GC content profile of the *P. polyspora*, *B. graminis* f. sp. *hordei*, *M. brunnea*, and *R. commune* genomes. GC content (x axis [%]) is plotted against the respective portion of the genome (y axis [%]). (B and C) RIP index analysis for repetitive sequences of the four genomes. Shown as box plots are the TpA/ApT ratio (B, y axis) and the (CpA + TpG)/(ApC + GpT) ratio (C, y axis) for three different TE families (Copia, Gypsy, and Tad1 [x axis]). The blue line depicts the thresholds set from *N. crassa* (0.89 and 1.03, respectively [37]), while the red line indicates the threshold values obtained by the non-TE-containing genomic sequences of the respective genomes. (D) Divergence analysis for the TEs in the *P. polyspora* genome. The histogram illustrates the total sequence length (y axis [bp]) with a given nucleotide sequence divergence (x axis [%]) for different types of TEs according to the color code in the legend shown on the right.

*Ascobolus immersus* and *Neurospora crassa* (32–35). Nevertheless, since these genes could have escaped the annotation process, or they could reside in genomic sequences that either had been removed during filtering or had not been fully assembled, we additionally searched for genomic sequences that bear characteristic RIP signatures (i.e., overrepresentation of certain dinucleotide repeats).

Initially we explored whether the *P. polyspora* draft genome has AT isochores, a typical feature of RIP-containing genomes such as in the case of *Leptosphaeria maculans* (36). We found that neither the *P. polyspora* nor the *B. graminis* f. sp. *hordei* genome contains AT-rich isochores (Fig. S2A). However, we observed that the intensity of the AT signature in genomes of other Leotiomyces that contain the genes necessary for RIP varies (see Fig. S5 in the supplemental material), with two exemplary cases for the presence of AT isochores being represented by *Marssonina brunnea* and *Rhynchosporium commune* (Fig. 2A). We proceeded by calculating two indices for these four genomes that could be informative regarding the presence of RIP. These two indices—TpA/ApT and (CpA + TpG)/(ApC + GpT)—have been used previously in *N. crassa* to detect signatures of RIP in repetitive sequences (37). They provide a measure of the prevalence and/or depletion of certain dinucleotides that are known results of RIP, while the respective baseline frequencies are calculated from nonrepetitive genomic sequences of the same genome. In the case of *N. crassa*, sequences with an TpA/ApT index higher than 0.89 and/or an (CpA + TpG)/(ApC + GpT) index lower than 1.03

suggest a biased frequency of AT dinucleotides caused by RIP (37). The baseline frequencies may vary between different species, as expected by the different overall nucleotide frequency of their genomes. In the genomes of *B. graminis* f. sp. *hordei* and *P. polyspora*, which seemingly lack RIP-related genes (see above), these indices likewise point to an absence of RIP. In contrast, respective values for *M. brunnea* and *R. commune* indicate the presence of RIP sequences, which is in agreement with the presence of AT-rich isochores and the genes of the RIP machinery in these genomes (Fig. 2B and C). Repetitive sequences that deviate from the set thresholds in *B. graminis* f. sp. *hordei* and *P. polyspora* could be relics of ancient RIP events, as has been previously suggested (38). Interestingly, the majority of the TEs in *P. polyspora* show high nucleotide sequence divergence (~30 to 40% [Fig. 2D]), in contrast to *B. graminis* f. sp. *hordei*, where recent TE bursts have been observed, resulting in highly similar (>90% sequence identity) TE copies (12).

**Powdery mildew genomes exhibit a lineage-specific loss of conserved ascomycete genes.** Next, we sought to determine if a set of conserved ascomycete genes (CAGs) that were previously found to be missing in the genome of the barley PM fungus (11) could be identified in the annotation of the *P. polyspora* draft genome. In addition, we surveyed additional PM, leotiomycete, and ascomycete proteomes to reevaluate the conservation of these proteins throughout the ascomycete lineage.

Interestingly, a major portion of these genes (61 out of 82) could be detected in the *P. polyspora* draft genome (Fig. 3A), in contrast to other PMs in which the presence of these genes is low but somewhat variable. For example, in the *B. graminis* f. sp. *hordei* genome, only 16 out of 82 CAGs were found. The presence of 16 genes that were considered to be absent in the early versions of the *B. graminis* f. sp. *hordei* reference genome (11) might be explained by its recently improved assembly and annotation (12). Some of the genes found to be present in *P. polyspora* are critical for common biochemical pathways such as glutathione metabolism (Fig. 3A). However, the preservation of genes in *P. polyspora* does not apply to all otherwise widely conserved functional modules. For example, the RIP mechanism is lacking (see above), and the number of genes encoding carbohydrate-active enzymes (CAZymes), which are abundant in close relatives of PMs (e.g., in *Botrytis cinerea* and *Sclerotinia sclerotiorum*), is comparatively low (Fig. 3B; Table S1F). Notably, the results of this analysis indicate that the loss of some of these conserved genes might have happened independently for the different PM sublineages (e.g., for the homologs of YHL016C and YIR023W or for YGL202W [Fig. 3A]), while others were seemingly lost prior to the diversification of the PMs (e.g., for the homologs involved in glutamate metabolism [Fig. 3A]). In order to reduce the likelihood of false positives originating from the integration of sequences from other fungal species in the assembly, we also inspected the origin of the putative *P. polyspora* CAGs by BLAST analysis with the nr database. All returned with a best hit to leotiomycete sequences.

In addition, we found that beyond a number of unique Pfam-annotated functional domains that can be detected in the genome of *P. polyspora* compared to that of *B. graminis* f. sp. *hordei* (Table S1G), there is a considerable fold difference (>3) in the presence of 27 Pfam domains in *P. polyspora* compared to *B. graminis* f. sp. *hordei* (Fig. 3C). Particularly noteworthy in this context are the flavin-binding monooxygenase-like and glucose-methanol-choline (GMC) oxidoreductase functional domains, which each show an >8-fold-increased presence in relation to *B. graminis* f. sp. *hordei* (Fig. 3C). In contrast, in comparison to the *B. graminis* f. sp. *hordei* genome the *P. polyspora* genome appears to be depleted for genes encoding members of the peptidase family S41 (>10-fold-lower content than in *B. graminis* f. sp. *hordei* [Fig. 3C]). This comparison also emphasizes some of the unique aspects of the *B. graminis* f. sp. *hordei* genome, such as the expansion of genes encoding proteins with Sgk2 domains (superfamily SSF56112 [39]), which cannot be observed to the same extent in the other PM genomes (see Fig. S6 in the supplemental material).

***P. polyspora* has a compact predicted secretome with a low number of RNase-like SPs.** We identified 261 SP candidates, out of which 193 had and 68 lacked a Pfam





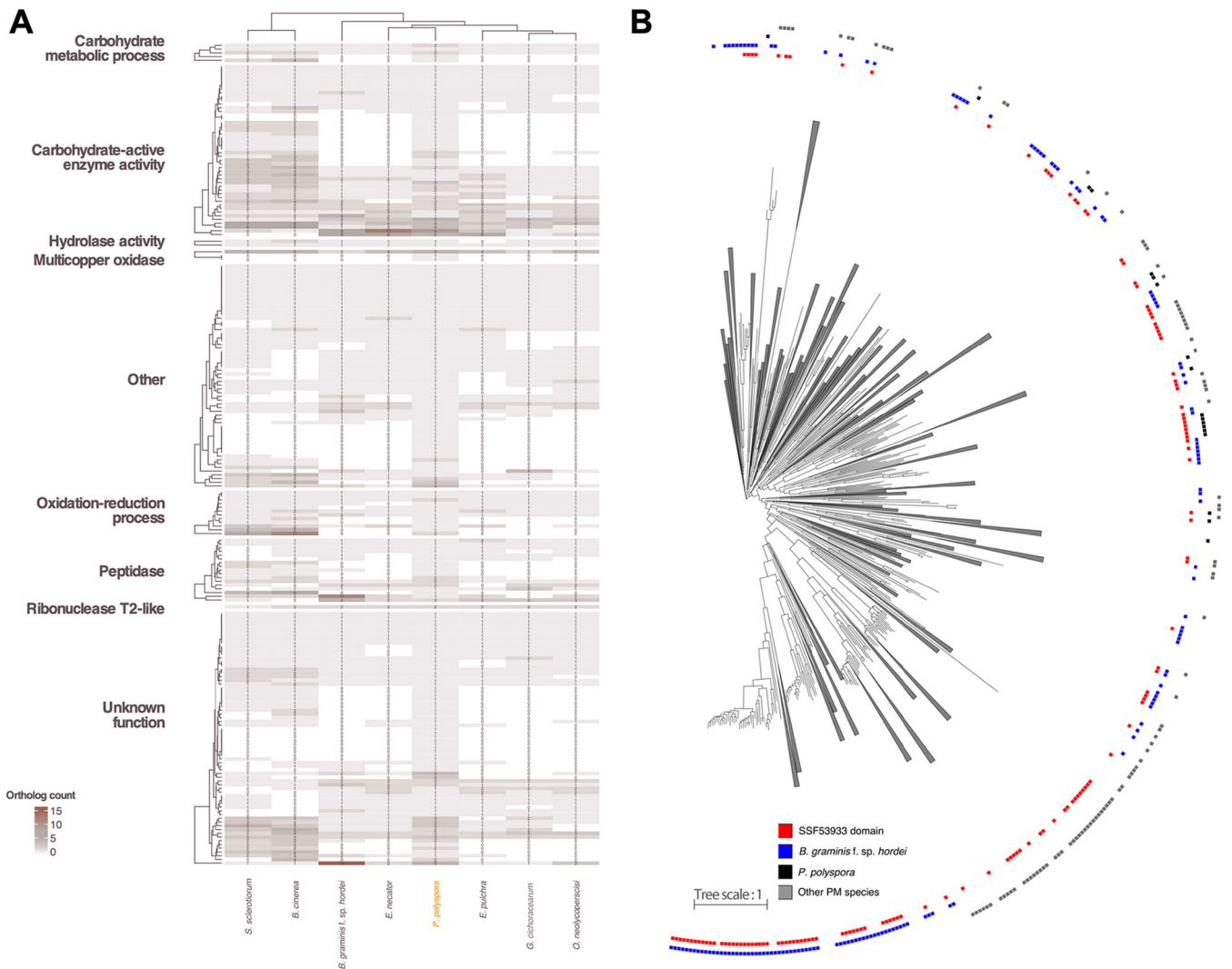


**FIG 4** Comparative analysis of the *P. polyspora* secretome. (A) Heat map depicting the differences in the SP gene content of the publicly accessible PM genomes and the genomes of two related leotiomycete species, *S. sclerotiorum* and *B. cinerea*, in comparison to *P. polyspora* according to the color code shown in the bottom left corner. The description of the functional categories of the orthogroups is based on Pfam. The cladograms are the result of hierarchical clustering. (B) Maximum likelihood phylogenetic tree (phylogram) of 1,227 putative SPs with no Pfam annotation from the predicted proteomes of *B. graminis f. sp. hordei*, *P. polyspora*, *E. necator*, *Erysiphe pulchra*, *Oidium neolycopersici*, and *Golovinomyces cichoracearum*. Branches that do not contain any RNase-like domain-containing proteins (superfamily SSF53933) were collapsed. The category “other PM species” indicated by gray boxes includes *E. necator*, *E. pulchra*, *O. neolycopersici*, and *G. cichoracearum*. Branches with bootstrap values lower than 60% were trimmed.

secretome of *P. polyspora* likewise contains RNase-like domain-carrying proteins (Inter-Pro accession no. SSF53933, PF06479, and PF00445) and whether there is a potential phylogenetic relationship of such proteins with respective homologs in other PMs. We identified only two proteins carrying a recognizable RNase-related domain, which is a surprisingly low number compared to *B. graminis f. sp. hordei* (86 members [12]). We additionally searched for gene models that were excluded from the final annotation (*ab initio* unsupported calls), and we were able to identify 13 additional genes coding for RNase-like SPs (domain accession no. SSF53933), which again is still a substantially lower number than in *B. graminis f. sp. hordei*. In the other non-*Blumeria* PM species, a similarly low number of secreted RNase-like proteins can be identified (3 to 19 members [Table S1H]), which suggests that there might be a *Blumeria*-specific expansion of this gene/protein family. Interestingly, after ortholog clustering of the mature (signal peptide removed) peptide sequences of the SPs, additional candidate SPs were found to exhibit sequence similarity to these proteins, despite not having a recognizable RNase-like domain (see Fig. S7 in the supplemental material).

In nearly all PM species examined here, family-specific expansions of genes encoding RNase-like SPs can be observed, and in addition, these RNase-like proteins are spread throughout different orthogroups (Fig. S7), suggesting a polyphyletic origin. We generated a maximum likelihood phylogenetic tree using all PM SP candidates with no Pfam domain (Fig. 4B), which further supports the notion that these RNase-like SPs are very diverse and potentially not of monophyletic origin. However, it has been recently suggested that despite the fact that they exhibit a severely eroded primary amino acid sequence similarity, the respective proteins may share an ancestor, as evidenced by a conserved intron position in the respective genes (42).

## DISCUSSION

**A natural leaf epiphytic metapopulation sample permits the assembly of a complex eukaryotic draft genome.** As a member of the taxonomic group of PM fungi, *P. polyspora* is believed to be an obligate biotrophic organism that cannot be cultured *in vitro*. Since the fungus is a pathogen of a tree species (*Quercus serrata*) that is native to eastern Asia, its propagation in pure culture would represent a formidable task. We thus took advantage of natural *P. polyspora*-infected leaf samples in the context of our project. Cellulose acetate peelings captured the leaf epiphytic microbiota of these samples and enabled the enrichment of sufficient biomass to allow genomic DNA extraction, sequencing, and assembly of a *P. polyspora* draft genome comprised of 495 high-confidence scaffolds (Fig. S1B). Although this assembly is based on a natural microbial metapopulation, k-mer and read depth coverage (Fig. S1C and D), sequence relatedness of the annotated genes (Table S1A), results of the BUSCO analysis (Table S1B), and the outcome of a multilocus phylogeny (Fig. 1A) support the notion that our assembly is of sufficient completeness and quality to allow downstream analyses. Inherent to studies based on natural metapopulation samples, we acknowledge that we cannot fully rule out contaminations and assembly artifacts, which to some extent limits the explanatory power of our study.

**Coevolutionary pace and life cycle attributes might drive genome plasticity in PMs.** Little is currently known about the biology of *P. polyspora*, which seems to propagate exclusively via ascospores produced during sexual reproduction, lacking a recognized asexual morph (i.e., conidiophores and conidia [22, 24]) and thus the asexual part of the typical PM life cycle. Accordingly, its precise host range, its mode of infection, the duration of its life cycle, and whether it represents indeed a homo- or heterothallic species remain to be explored.

At ~29 Mb, the assembled draft genome of this species is approximately 4-fold smaller than the average genome of other sequenced PM fungi (12, 16, 18, 19) and even smaller than the average filamentous ascomycete genome (~37 Mb [43]). Accordingly, it lacks the distinct abundance of repetitive elements that otherwise characterizes genomes of PM species (Table S1C), but shares with them a comparatively low gene number (~6,000) and a noncompartmentalized organization (Fig. 1C; Fig. S3) (12). These inferences derive from the analysis of the assembled high-confidence contigs obtained from our metagenomic *Q. serrata* sample and thus, in principle, could reflect a considerable underrepresentation of the *P. polyspora* genome. The number of repetitive elements could also be underestimated, as this happens even in assemblies of “streamlined” genomes (44). However, results of k-mer analysis support the estimated genome size via an independent approach, and the low average size of the intergenic space (Fig. 1A) additionally corroborates the idea of a very compact genome. Furthermore, gene number and results of the BUSCO analysis indicate that the majority (~94%) of the typical PM gene space is covered by the high-confidence contigs. Even when taking into account the low-confidence contigs, the calculated genome size would not exceed 61 Mb—a value still 2-fold smaller than that of other sequenced PM fungi.

Notably, the draft genome is indicative of homothallism (self-fertilization) since we located characteristic genes of both mating types (MAT1-1 and MAT1-2) on a single contig (Fig. S4). This finding is surprising since the majority of PMs are considered to be

heterothallic (29), and therefore we expected that our sampling material containing sexual reproduction structures (chasmothecia) should recover discrete scaffolds representing both mating-type loci. Nevertheless, homothallism in PM fungi has been reported several times (29), although most of these reports lack molecular evidence. In contrast to the described homothallic *Plantago lanceolata* pathogen *Podosphaera plantaginis*, where both *MAT* idiomorphs likely exist as functional genes within the same genome (29), in *P. polyspora* the recovered *MAT* locus contains a seemingly intact *MAT1-2-1* and an apparently pseudogenized *MAT1-1-3* (Fig. S4). Moreover, a homolog of *MAT1-1-1*, supposed to be an indispensable feature of the *MAT1-1* mating type (30), seems to be completely absent. Thus, in *P. polyspora*, a joint *MAT1-1/MAT1-2* locus exists, but it appears as if one of the two idiomorphs (*MAT1-1*) became dispensable for sexual reproduction of this fungus. This scenario, where only one *MAT* idiomorph is sufficient for self-fertility, has been observed previously in ascomycetes (“same-sex mating” [45]), yet it is considered a rare occurrence (46). As in other homothallic ascomycetes and their closely related heterothallic counterparts (47), synteny between the *P. polyspora* *MAT1-1/MAT1-2* locus and the *MAT* loci of the closely related heterothallic *B. graminis* f. sp. *hordei* is poorly conserved. This reported lack of synteny in homothallic loci compared to closely related heterothallic species might also explain why the arrangement of the *P. polyspora* locus is different from the suggested locus of *P. plantaginis* (29).

Interestingly, the *P. polyspora* genome retained many genes that were lost in more recently evolved PMs, but similarly to the latter lacks genes associated with the RIP genome defense mechanism (Fig. 2A to C and Fig. 3A). This finding suggests that the RIP pathway was abandoned in an early progenitor species of the PM lineage at least 80 to 90 million years ago prior to the separation of the *Parauncinula* genus from the other PMs (23). The absence of RIP but maintenance of a compact genome in the case of *P. polyspora* implies that the propagation of TEs in the genomes of the Erysiphales might be restrained by other mechanisms and/or suppressed by certain attributes of the *Parauncinula* life cycle. A plausible hypothesis is that the sexual propagation in *Parauncinula* might contribute to the maintenance of a lean genome, in comparison to the mainly asexually propagating species of the genera *Golovinomyces*, *Blumeria*, *Podosphaera*, and *Erysiphe* (10). This idea would support the overall assumption that sexual recombination can limit the uncontrolled proliferation of TEs while at the same time help in spreading beneficial mutations (48). Nevertheless, examples of fungal species lacking sexual propagation, RIP, and an abundance of TEs exist (49), indicating that broad generalizations cannot be easily made.

On the other hand, it might be argued that the selection pressure in the *P. polyspora*-*Q. serrata* interaction is comparatively low. In cases where PMs infect annual, agriculturally relevant hosts, breeding and growing of cultivars with novel resistance specificities as well as crop protection measures place massive selection pressure on pathogen populations. A particularly plastic and rapidly evolving genome (opposed to the case of *P. polyspora*) should be an advantage during adaptation and survival of crop pathogens. *P. polyspora* likely causes monocyclic infections with a much lower propagation rate, since the lack of conidiophores does not allow for the rapid and profuse aerial dispersal of conidia and multiple infection cycles per year—as, for example, in *B. graminis*. In addition, the host, *Q. serrata*, has a long, perennial life cycle, leading to a limited ability to evade a pathogen with a rapid turnover of resistance genes. Also, its genetically diverse local populations (50) may offer a less selective environment than the hosts in uniform agricultural settings (51, 52). In this scenario, both partners (*P. polyspora* and *Q. serrata*) might be locked in an arms race, albeit at a much slower pace compared to the interactions between many annual plant species and the respective PMs. This could be echoed by the *P. polyspora* genome, in which the relative scarcity of TEs does not offer a template for rapid evolution of virulence genes by duplications (Table S1D), small-scale rearrangements, or deletions, as has been proposed for *B. graminis* f. sp. *hordei* and *B. graminis* f. sp. *tritici* (12, 16, 53). The smaller secretome and the number of unique secreted proteins with no known functional

domains (i.e., typical effector candidates) in *P. polyspora* can also be considered as support for this hypothesis. While definitely this result originates in part from the lack of transcriptomic data, it is now a more general observation that dicot-infecting PM have more compact secretomes, presumably because of different selection processes than those acting on the grass-infecting species (i.e., negative versus positive selection [40]). Our data, together with results from recent studies on genomes of additional dicot-infecting PM species (18, 19, 40), indicate that the expansion of the total amount of virulence genes or particular families thereof might be specific to PM lineages that emerged recently and are under high selection pressure.

**Gene functional reduction and family expansion are an ongoing process in PMs.** The *P. polyspora* draft genome reveals that more CAGs are present in an ancestral than in derived PM species and also that the respective gene losses are unequal (Fig. 3A). Recent studies indicate that this likewise extends to CAGs not included here (18), as for example, shown by the absence of a part of the RNA interference (RNAi) machinery in the grapevine PM pathogen *Erysiphe necator* (54). Since the remaining CAGs are dispersed in the genome, it is unlikely that their absence is the result of some large-scale genome reduction: e.g., the loss of a single chromosome. Instead, it seems to be in part stochastic, possibly due to local illegitimate recombination activity caused by TE insertions adjacent to the genes (53). The eventual fixation of these losses as observed in the different PM lineages could be a driver of the subsequent strict association of these species with a low number of specific hosts and their spatial and reproductive isolation from other PMs. It may also favor the succeeding loss of additional functional categories (Fig. 3B and C and Fig. 4A) that are related to virulence (i.e., peptidases, CAZymes, and redox enzymes) but no longer needed to that extent in a highly specialized host environment. This might also apply to asexual reproduction (conidiospore formation), which appears to be absent in species of the genera *Parauncinula*, *Brasiliomyces*, and *Typhulochaeta* within the Erysiphales (10). Taken together, the pattern of present/absent genes in the PM genomes thus appears to result from a mixture of divergent, convergent, and individual gene losses.

We hypothesize that in PMs, extinction by genome erosion is avoided by the compensatory lineage-specific expansion of gene families that support virulence (e.g., encoding effector proteins) or other physiological processes. Two examples that were identified here are secreted RNase-like proteins (Fig. 4B; Fig. S7) and Sgk2-type serine/threonine protein kinases (Fig. S6), which appear to have specifically multiplied their numbers in *B. graminis* f. sp. *hordei*. Some RNase-like SPs have been previously shown to be involved in virulence and/or to be recognized by the plant host (17, 42, 53, 55–57), while the role of Sgk2-type serine/threonine protein kinases in PM biology remains elusive (39). Yet in other fungal pathogens, it is speculated that kineome expansion is related to environmental and stress responses (58).

**A hypothetical model for the evolutionary adaptation of powdery mildew fungi.** Based on the data available so far, we hypothesize the following scenario, which is summarized in Fig. 5. An ancestor of the PM lineage experienced the loss of the RIP machinery and a limited loss of CAGs. After diverging from the other PM lineages, *P. polyspora* was subject to a loss of the asexual life cycle, the establishment of homothallism, and the expansion of particular protein families (e.g., monooxygenases and oxidoreductases). The other PM genomes, derived after this early split, underwent a TE-associated genome expansion and the loss of additional CAGs. Separate lineages strictly associated with certain monocot or dicot hosts were established, and different modes of infection (epiphytic versus endophytic) evolved based on a reoccurring pattern of loss and/or expansion of virulence-related and other gene families. This pattern is exemplified by the specific expansion of RNase-like effector proteins and Sgk2 kinases in the monocot-infecting lineage, but also by the unequal loss of CAGs and the reported expansion of other functional families in dicot-infecting PMs (e.g., cation binding proteins [18]).

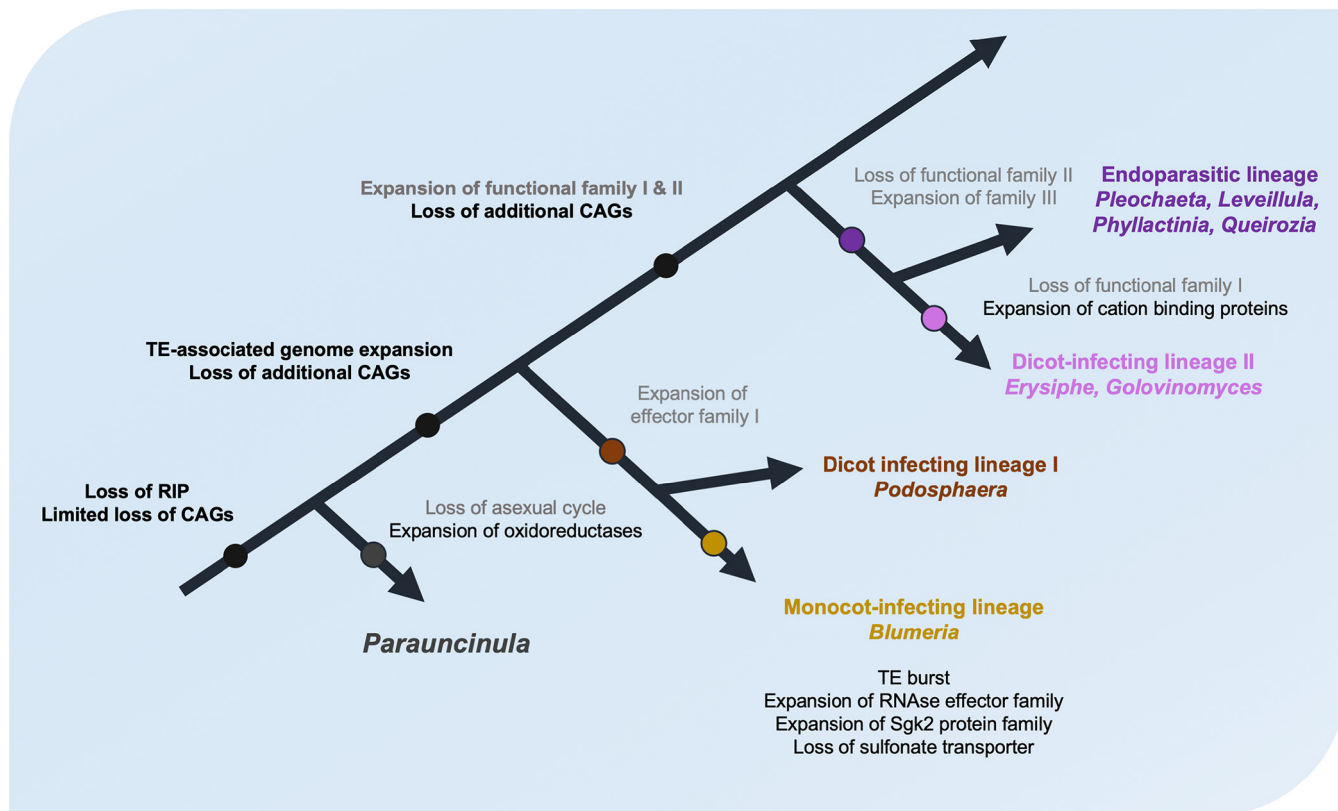


**FIG 5** A hypothetical model for the evolution of the PM fungi. A simplified and schematic phylogenetic tree illustrating the evolution of PM fungi is shown. Genomic features for which some evidence is provided by the present work and previous studies are shown in black, while hypothetical losses and expansions are depicted in gray, and major/driving events for adaptation to new hosts are highlighted in boldface.

## MATERIALS AND METHODS

**Genomes and proteomes used in this study.** The genomes and proteomes used in this study are listed in Table 2.

**Sampling and genomic DNA extraction.** Infected leaves of a single *P. polyspora*-infected *Q. serrata* tree were collected in 2017 in Torimiyama Park, Haibara, Uda-shi, Nara Prefecture, Japan (N34.543809, E135.944306). The leaf samples were dipped in 5% (wt/vol) cellulose acetate-acetone solution and then placed to dry. The cellulose was peeled off using forceps, and the sample was ground in liquid nitrogen with a mortar and pestle. The resulting cellulose fragments with fungal structures attached were transferred to 2-ml tubes, and genomic DNA extraction was performed as described in reference 15. Afterwards, small DNA fragments (<100 bp) were removed using AMPure XP beads (Beckman Coulter, Krefeld, Germany), and the quantity and quality of the DNA were assessed using a NanoDrop spectrophotometer (Thermo Fisher Scientific, Darmstadt, Germany) and a Qubit fluorometer (Thermo Fisher).

**Genome sequencing, assembly, and functional annotation.** Illumina library preparation (TruSeq DNA Nano; Illumina) and genomic sequencing were performed by CeGaT GmbH in Tübingen, Germany. The library was sequenced on the NovaSeq 6000 platform and resulted in 163.1 million paired raw reads ( $2 \times 150$  bp, a total of 24.6 Gbp of data). The reads were assessed for their content of leotiomycete sequences using MG-RAST (MG-RAST identification no. f5bdd547896d676d343830363131372e33) (59).

The pipeline followed to assemble the genome is briefly presented in Fig. S1A. In more detail, the adapters were trimmed with Skewer (60) and then passed to BFC (-b 32 -k 25 -t 10) (61) for error correction and removal of singleton k-mers. The corrected reads were then assembled with SPAdes v3.11.1 (--only-assembler -k 31,51,71,91,111 --meta) (62). In order to remove bacterial and eukaryotic contaminating sequences from the resulting scaffolds, the sequences were initially searched by BLAST against a set of 3,837 plant-associated bacterial genomes ([http://labs.bio.unc.edu/Dangl/Resources/gfobap\\_website/index.html](http://labs.bio.unc.edu/Dangl/Resources/gfobap_website/index.html); 63). The resulting scaffolds were filtered based on their depth (cutoff of  $>20\times$  [Fig. S1C]) and the homology of their annotations to the Leotiomycetes. For the exclusion based on the leotiomycete homology, after the annotation (see below) the predicted genes were used for homology search against the NCBI nr protein database (last accessed November 2017) using BLAST+ v2.3.0 (64). Scaffolds where the two most frequent hits to the nr belonged to the Leotiomycetes were deemed as high-confidence scaffolds, while the rest were placed in the low-confidence group. The high-confidence scaffolds were assessed for coverage of the gene space using BUSCO v1.22 (26), and an additional size estimation based on k-mer abundance was provided using Jellyfish v2.2.10 (27) with reads that aligned only to the high-confidence contigs and a k-mer option for 31 bp (-m 31).

**TABLE 2** Genomes and proteomes used in this study

Data set	Accession no./release	Reference/website
Nonredundant protein database (nr)	Downloaded 28 August 2017	<a href="ftp.ncbi.nlm.nih.gov">ftp.ncbi.nlm.nih.gov</a>
UniProt	2016_05	<a href="http://www.uniprot.org/downloads">http://www.uniprot.org/downloads</a>
<i>Aspergillus niger</i> CBS 513.88	GCF_000002855.3	NCBI
<i>Blumeria graminis</i> f. sp. <i>tritici</i> 96224	GCA_000418435.1	NCBI
<i>Blumeria graminis</i> f. sp. <i>hordei</i> K1	GCA_000401615.1	NCBI
<i>Blumeria graminis</i> f. sp. <i>hordei</i> DH14	GCA_900239735.1	<a href="https://genome.jgi.doe.gov/Blugr2/Blugr2.info.html">https://genome.jgi.doe.gov/Blugr2/Blugr2.info.html</a>
<i>Botrytis cinerea</i> B05.10	GCF_000143535.1	NCBI
<i>Colletotrichum graminicola</i> M1.001	GCF_000149035.1	NCBI
<i>Erysiphe necator</i>	GCA_000798715.1	NCBI
<i>Erysiphe pulchra</i>	GCA_0002918395.1	NCBI
<i>Fusarium oxysporum</i>	GCA_000149955.2	NCBI
<i>Glarea lozoyensis</i> 20868	GCF_000409485.1	NCBI
<i>Golovinomyces cichoracearum</i>	<a href="#">GSE85906</a> (GEO)	NCBI
<i>Magnaporthe oryzae</i> 70-15	GCF_000002495.2	NCBI
<i>Marssonina brunnea</i> f. sp. MBm1	GCF_000298775.1	NCBI
<i>Neurospora crassa</i>	p3_p13841	<a href="ftp://ftpmips.gsf.de/fungi/">ftp://ftpmips.gsf.de/fungi/</a>
<i>Oidiodendron maius</i>	GCA_000827325.1	NCBI
<i>Oidium neolycopesci</i>	<a href="#">GSE85906</a> (GEO)	NCBI
<i>Penicillium digitatum</i>	GCA_000315645.2	NCBI
<i>Phialocephala scopiformis</i>	GCF_001500285.1	NCBI
<i>Phialocephala subalpina</i>	GCA_900073065.1	NCBI
<i>Pseudogymnoascus destructans</i>	GCF_000184105.1	NCBI
<i>Pseudogymnoascus verrucosus</i>	GCF_001662655.1	NCBI
<i>Quercus suber</i>	GCF_002906115.1	NCBI
<i>Rhynchosporium agropyri</i>	GCA_900074905.1	NCBI
<i>Rhynchosporium commune</i>	GCA_900074885.1	NCBI
<i>Rhynchosporium secalis</i>	GCA_900074895.1	NCBI
<i>Sclerotinia borealis</i>	GCA_000503235.1	NCBI
<i>Sclerotinia sclerotiorum</i> 1980	GCF_000146945.1	NCBI
<i>Verticillium dahliae</i> VdLs.17	GCF_000150675.1	NCBI
<i>Zymoseptoria tritici</i> IPO323	GCF_000219625.1	NCBI

For the annotation of the scaffolds, we followed the same pipeline as described before (12) using MAKER (65). The data sets provided as evidence are listed in Table 2. Afterwards functional annotation was performed using InterProScan v5.19-58.0 (66) and HMMER v3.1 (67) with dbCAN v6 (68) for the identification of CAZymes specifically. Putatively secreted proteins with no transmembrane domains were identified using SignalP v4.1 (69) and TMHMM v2.0c (70). Mating-type genes were identified by bidirectional BLAST searches (64) using BLASTP and TBLASTN with an E value cutoff of  $10e^{-5}$ .

**Analysis of repetitive sequences.** Repetitive sequences were identified using RepeatMasker v4.0.6 (<http://www.repeatmasker.org>) using Repbase as a database (last accessed 9 June 2016). Subsequently, a repeat landscape was generated for *P. polyspora* as described before (12). GC composition of the selected leotiomycete genomes and dinucleotide frequencies were calculated using OcculterCut v1.1 (71) and RIPCAL v2 (72), respectively.

**Orthogroup inference, phylogeny, and nucleotide polymorphisms.** Identification of ortholog groups and generation of gene family trees were performed using OrthoFinder v1.1.2 (73). The maximum likelihood phylogenetic trees based on putatively secreted proteins with no Pfam annotation or on single-copy orthologs were generated using FastTree v2.1.10 (74) after alignment of the protein sequences with MAFFT v7.310 (75). Figures of the trees were generated using iTOL (76) and are available at <https://itol.embl.de/shared/lambros2>. CAG search using the proteomes listed above was performed using BLASTP (64) with an E value threshold of  $10e^{-5}$ .

In order to discover the number of single nucleotide polymorphisms in the *P. polyspora* genome assembly, we initially mapped the reads using BWA-MEM v0.7.15-r1140 (77). The resulting sam file was processed (conversion to bam, sorting) with Picard tools v2.8.2 (<http://broadinstitute.github.io/picard>), and then polymorphisms were identified using samtools mpileup and bcftools (v0.1.19) (78) and filtered with SnpSift v4.3i (QUAL  $\geq 20$  && DP  $> 3$  && MQ  $> 50$ ) (79).

**Data availability.** Corresponding R scripts and associated files (phylogenetic trees, tables, etc.) used for generating figures used in this article have been deposited in GitHub at [https://github.com/lambros-f/paraun\\_2018](https://github.com/lambros-f/paraun_2018). In all software utilized for the analysis, if no explicit settings are mentioned, then the defaults were used. The data set, including raw reads and the assembled genome used here, has been deposited in the European Nucleotide Archive (ENA) under accession no. [PRJEB29715](#).

## SUPPLEMENTAL MATERIAL

Supplemental material for this article may be found at <https://doi.org/10.1128/mBio.01692-19>.

**FIG S1**, PDF file, 1 MB.

**FIG S2**, PDF file, 1.3 MB.

**FIG S3**, PDF file, 0.2 MB.

**FIG S4**, PDF file, 0.4 MB.

**FIG S5**, PDF file, 0.7 MB.

**FIG S6**, PDF file, 0.3 MB.

**FIG S7**, PDF file, 0.3 MB.

**TABLE S1**, XLSX file, 2.6 MB.

## ACKNOWLEDGMENTS

We acknowledge the contribution of Diána Seress to sample preparation.

The authors declare that they have no competing interests.

This work was supported by a grant of the Deutsche Forschungsgemeinschaft (DFG)-funded Priority Program SPP1819 (Rapid Evolutionary Adaptation—Potential and Constraints) to R.P. (PA 861/14-1). Additionally, this study was partly supported by a grant of the Australia-Germany Joint Research Co-Operation Scheme and the program PPP Australia 2019 funded by the German Academic Exchange Service (DAAD). The bioinformatic analysis was performed with computing resources granted by RWTH Aachen University under project no. rwth0146.

R.P. and L.F. conceived the study and drafted the manuscript. S.T. did the field sampling, and M.Z.N. and L.K. contributed to sample preparation. L.F. and M.Z.N. performed the experiments. L.F. analyzed the data. L.F., M.B., and S.K. analyzed the mating loci. R.P., S.T., and L.K. provided conceptual advice. All authors edited, read, and approved the final version of the manuscript.

## REFERENCES

1. Gladieux P, Ropars J, Badouin H, Branca A, Aguilera G, de Vienne DM, La Rodríguez de Vega RC, Branco S, Giraud T. 2014. Fungal evolutionary genomics provides insight into the mechanisms of adaptive divergence in eukaryotes. *Mol Ecol* 23:753–773. <https://doi.org/10.1111/mec.12631>.
2. Dong S, Raffaele S, Kamoun S. 2015. The two-speed genomes of filamentous pathogens: waltz with plants. *Curr Opin Plant Biol* 35:57–65. <https://doi.org/10.1016/j.copbi.2015.09.001>.
3. Brown J. 2015. Durable resistance of crops to disease: a Darwinian perspective. *Annu Rev Phytopathol* 53:513–539. <https://doi.org/10.1146/annurev-phyto-102313-045914>.
4. Raffaele S, Kamoun S. 2012. Genome evolution in filamentous plant pathogens: why bigger can be better. *Nat Rev Microbiol* 10:417–430. <https://doi.org/10.1038/nrmicro2790>.
5. Mori Y, Sato Y, Takamatsu S. 2000. Evolutionary analysis of the powdery mildew fungi using nucleotide sequences of the nuclear ribosomal DNA. *Mycologia* 92:74. <https://doi.org/10.2307/3761452>.
6. Spanu PD, Panstruga R. 2012. Powdery mildew genomes in the crosshairs. *New Phytol* 195:20–22. <https://doi.org/10.1111/j.1469-8137.2012.04173.x>.
7. Cabrera MG, Álvarez RE, Takamatsu S. 2018. Morphology and molecular phylogeny of *Brasiliomyces malachrae*, a unique powdery mildew distributed in Central and South America. *Mycoscience* 59:461–466. <https://doi.org/10.1016/j.myc.2018.04.003>.
8. Troch V, Audenaert K, Wyand RA, Haesaert G, Höfte M, Brown JK. 2014. *Formae speciales* of cereal powdery mildew: close or distant relatives? *Mol Plant Pathol* 15:304–314. <https://doi.org/10.1111/mpp.12093>.
9. Braun U, Cook RTA. 2012. Taxonomic manual of the Erysiphales (powdery mildews). CBS biodiversity series, vol 11. CBS-KNAW Fungal Biodiversity Centre, Utrecht, The Netherlands.
10. Glawe DA. 2008. The powdery mildews: a review of the world's most familiar (yet poorly known) plant pathogens. *Annu Rev Phytopathol* 46:27–51. <https://doi.org/10.1146/annurev.phyto.46.081407.104740>.
11. Spanu PD, Abbott JC, Amselem J, Burgis TA, Soanes DM, Stüber K, van Themaat EVL, Brown JKM, Butcher SA, Gurr SJ, Lebrun MH, Ridout CJ, Schulze-Lefert P, Talbot NJ, Ahmadijad N, Ametz C, Barton GR, Benjdia M, Bidzinski P, Bindschedler LV, Both M, Brewer MT, Cadle-Davidson L, Cadle-Davidson MM, Collemare J, Cramer R, Frenkel O, Godfrey D, Harriman J, Hoede C, King BC, Klages S, Kleemann J, Knoll D, Koti PS, Kreplak J, Lopez-Ruiz FJ, Lu XL, Maekawa T, Mahanil S, Micali C, Milgroom MG, Montana G, Noir S, O'Connell RJ, Oberhaensli S, Parlange F, Peder-
12. Frantzeskakis L, Kracher B, Kusch S, Yoshikawa-Maekawa M, Bauer S, Pedersen C, Spanu PD, Maekawa T, Schulze-Lefert P, Panstruga R. 2018. Signatures of host specialization and a recent transposable element burst in the dynamic one-speed genome of the fungal barley powdery mildew pathogen. *BMC Genomics* 19:27. <https://doi.org/10.1186/s12864-018-4750-6>.
13. Wicker T, Oberhaensli S, Parlange F, Buchmann JP, Shatalina M, Roffler S, Ben-David R, Doležal J, Simková H, Schulze-Lefert P, Spanu PD, Bruggmann R, Amselem J, Quesneville H, van Themaat EVL, Paape T, Shimizu KK, Keller B. 2013. The wheat powdery mildew genome shows the unique evolution of an obligate biotroph. *Nat Genet* 45:1092–1096. <https://doi.org/10.1038/ng.2704>.
14. Bindschedler LV, Panstruga R, Spanu PD. 2016. Mildew-omics: how global analyses aid the understanding of life and evolution of powdery mildews. *Front Plant Sci* 7:123. <https://doi.org/10.3389/fpls.2016.00123>.
15. Feehan JM, Scheibel KE, Bourras S, Underwood W, Keller B, Somerville SC. 2017. Purification of high molecular weight genomic DNA from powdery mildew for long-read sequencing. *J Vis Exp* <https://doi.org/10.3791/55463>.
16. Müller MC, Praz CR, Sotiropoulos AG, Menardo F, Kunz L, Schudel S, Oberhänsli S, Poretti M, Wehrli A, Bourras S, Keller B, Wicker T. 2018. A chromosome-scale genome assembly reveals a highly dynamic effector repertoire of wheat powdery mildew. *New Phytol* <https://doi.org/10.1111/nph.15529>.
17. Lu X, Kracher B, Saur IML, Bauer S, Ellwood SR, Wise R, Yaeno T, Maekawa T, Schulze-Lefert P. 2016. Allelic barley MLA immune receptors recognize sequence-unrelated avirulence effectors of the powdery mildew pathogen. *Proc Natl Acad Sci U S A* 113:E6486–E6495. <https://doi.org/10.1073/pnas.1612947113>.
18. Wu Y, Ma X, Pan Z, Kale SD, Song Y, King H, Zhang Q, Presley C, Deng X, Wei C-I, Xiao S. 2018. Comparative genome analyses reveal sequence features reflecting distinct modes of host-adaptation between dicot and monocot powdery mildew. *BMC Genomics* 19:705. <https://doi.org/10.1186/s12864-018-5069-z>.
19. Jones L, Riaz S, Morales-Cruz A, Amrine KCH, McGuire B, Gubler WD, Walker MA, Cantu D. 2014. Adaptive genomic structural variation in the

- grape powdery mildew pathogen, *Erysiphe necator*. BMC Genomics 15: 1081. <https://doi.org/10.1186/1471-2164-15-1081>.
20. Menardo F, Wicker T, Keller B. 2017. Reconstructing the evolutionary history of powdery mildew lineages (*Blumeria graminis*) at different evolutionary time scales with NGS data. Genome Biol Evol 9:446–456. <https://doi.org/10.1093/gbe/evx008>.
  21. Menardo F, Praz CR, Wicker T, Keller B. 2017. Rapid turnover of effectors in grass powdery mildew (*Blumeria graminis*). BMC Evol Biol 17:223. <https://doi.org/10.1186/s12862-017-1064-2>.
  22. Takamatsu S, Limkaisang S, Braun U. 2005. Phylogenetic relationships and generic affinity of *Uncinula septata* inferred from nuclear rDNA sequences. Mycoscience 46:9–16. <https://doi.org/10.1007/S10267-004-0205-9>.
  23. Takamatsu S, Ninomi S, Cabrera de Álvarez MG, Álvarez RE, Havrylenko M, Braun U. 2005. *Caespitotheca* gen. nov., an ancestral genus in the Erysiphales. Mycol Res 109:903–911. <https://doi.org/10.1017/S0953756205003047>.
  24. Meeboon J, Siahaan SAS, Fujioka K, Takamatsu S. 2017. Molecular phylogeny and taxonomy of *Parauncinula* (Erysiphales) and two new species *P. polyspora* and *P. uncinata*. Mycoscience 58:361–368. <https://doi.org/10.1016/j.myc.2017.04.007>.
  25. Both M, Csukai M, Stumpf MPH, Spanu PD. 2005. Gene expression profiles of *Blumeria graminis* indicate dynamic changes to primary metabolism during development of an obligate biotrophic pathogen. Plant Cell 17:2107–2122. <https://doi.org/10.1105/tpc.105.032631>.
  26. Simão FA, Waterhouse RM, Ioannidis P, Kriventseva EV, Zdobnov EM. 2015. BUSCO: assessing genome assembly and annotation completeness with single-copy orthologs. Bioinformatics 31:3210–3212. <https://doi.org/10.1093/bioinformatics/btv351>.
  27. Marçais G, Kingsford C. 2011. A fast, lock-free approach for efficient parallel counting of occurrences of k-mers. Bioinformatics 27:764–770. <https://doi.org/10.1093/bioinformatics/btr011>.
  28. Debuchy R, Berteaux-Lecellier V, Silar P. 2010. Mating systems and sexual morphogenesis in ascomycetes, p 501–535. In Borkovich KA (ed), Cellular and molecular biology of filamentous fungi. American Society for Microbiology, Washington, DC.
  29. Tollenaere C, Laine A-L. 2013. Investigating the production of sexual resting structures in a plant pathogen reveals unexpected self-fertility and genotype-by-environment effects. J Evol Biol 26:1716–1726. <https://doi.org/10.1111/jeb.12169>.
  30. Brewer MT, Cadle-Davidson L, Cortesi P, Spanu PD, Milgroom MG. 2011. Identification and structure of the mating-type locus and development of PCR-based markers for mating type in powdery mildew fungi. Fungal Genet Biol 48:704–713. <https://doi.org/10.1016/j.fgb.2011.04.004>.
  31. Galagan JE, Selker EU. 2004. RIP: the evolutionary cost of genome defense. Trends Genet 20:417–423. <https://doi.org/10.1016/j.tig.2004.07.007>.
  32. Kouzminova E, Selker EU. 2001. *dim-2* encodes a DNA methyltransferase responsible for all known cytosine methylation in *Neurospora*. EMBO J 20:4309–4323. <https://doi.org/10.1093/emboj/20.15.4309>.
  33. Malagnac F, Wendel B, Goyon C, Faugeron G, Zickler D, Rossignol JL, Noyer-Weidner M, Vollmayr P, Trautner TA, Walter J. 1997. A gene essential for de novo methylation and development in *Ascomobolus* reveals a novel type of eukaryotic DNA methyltransferase structure. Cell 91:281–290. [https://doi.org/10.1016/S0092-8674\(00\)80410-9](https://doi.org/10.1016/S0092-8674(00)80410-9).
  34. Malagnac F, Grégoire A, Goyon C, Rossignol JL, Faugeron G. 1999. *Masc2*, a gene from *Ascomobolus* encoding a protein with a DNA-methyltransferase activity *in vitro*, is dispensable for *in vivo* methylation. Mol Microbiol 31:331–338. <https://doi.org/10.1046/j.1365-2958.1999.01177.x>.
  35. Freitag M, Williams RL, Kothe GO, Selker EU. 2002. A cytosine methyltransferase homologue is essential for repeat-induced point mutation in *Neurospora crassa*. Proc Natl Acad Sci U S A 99:8802–8807. <https://doi.org/10.1073/pnas.132212899>.
  36. Rouxel T, Grandaubert J, Hane JK, Hoede C, van de Wouw AP, Couloux A, Dominguez V, Anthouard V, Bally P, Bourras S, Cozijnsen AJ, Ciuffetti LM, Degraeve A, Dilmaghani A, Duret L, Fudal I, Goodwin SB, Gout L, Glaser N, Linglin J, Kema GHJ, Lapalu N, Lawrence CB, May K, Meyer M, Ollivier B, Poulain J, Schoch CL, Simon A, Spatafora JW, Stachowiak A, Turgeon BG, Tyler BM, Vincent D, Weissenbach J, Amselem J, Quesneville H, Oliver RP, Wincker P, Balesdent M-H, Howlett BJ. 2011. Effector diversification within compartments of the *Leptosphaeria maculans* genome affected by repeat-induced point mutations. Nat Commun 2:202. <https://doi.org/10.1038/ncomms1189>.
  37. Margolin BS, Garrett-Engle PW, Stevens JN, Fritz DY, Garrett-Engle C, Metzberg RL, Selker EU. 1998. A methylated *Neurospora* 5S rRNA pseudogene contains a transposable element inactivated by repeat-induced point mutation. Genetics 149:1787–1797.
  38. Amselem J, Lebrun M-H, Quesneville H. 2015. Whole genome comparative analysis of transposable elements provides new insight into mechanisms of their inactivation in fungal genomes. BMC Genomics 16:141. <https://doi.org/10.1186/s12864-015-1347-1>.
  39. Kusch S, Ahmadijeh N, Panstruga R, Kuhn H. 2014. *In silico* analysis of the core signaling proteome from the barley powdery mildew pathogen (*Blumeria graminis* f. sp. *hordei*). BMC Genomics 15:843. <https://doi.org/10.1186/1471-2164-15-843>.
  40. Liang P, Liu S, Xu F, Jiang S, Yan J, He Q, Liu W, Lin C, Zheng F, Wang X, Miao W. 2018. Powdery mildews are characterized by contracted carbohydrate metabolism and diverse effectors to adapt to obligate biotrophic lifestyle. Front Microbiol 9:3160. <https://doi.org/10.3389/fmicb.2018.03160>.
  41. Pedersen C, Ver Loren van Themaat E, McGuffin LJ, Abbott JC, Burgis TA, Barton G, Bindschedler LV, Lu X, Maekawa T, Weßling R, Cramer R, Thordal-Christensen H, Panstruga R, Spanu PD. 2012. Structure and evolution of barley powdery mildew effector candidates. BMC Genomics 13:694. <https://doi.org/10.1186/1471-2164-13-694>.
  42. Spanu PD. 2017. Cereal immunity against powdery mildews targets RNase-like proteins associated with Haustoria (RALPH) effectors evolved from a common ancestral gene. New Phytol 213:969–971. <https://doi.org/10.1111/nph.14386>.
  43. Mohanta TK, Bae H. 2015. The diversity of fungal genome. Biol Proced Online 17:8. <https://doi.org/10.1186/s12575-015-0020-z>.
  44. Thomma B, Seidl MF, Shi-Kunne X, Cook DE, Bolton MD, van Kan JAL, Faino L. 2016. Mind the gap; seven reasons to close fragmented genome assemblies. Fungal Genet Biol 90:24–30. <https://doi.org/10.1016/j.fgb.2015.08.010>.
  45. Alby K, Bennett RJ. 2011. Interspecies pheromone signaling promotes biofilm formation and same-sex mating in *Candida albicans*. Proc Natl Acad Sci U S A 108:2510–2515. <https://doi.org/10.1073/pnas.1017234108>.
  46. Billiard S, López-Villavicencio M, Devier B, Hood ME, Fairhead C, Giraud T. 2011. Having sex, yes, but with whom? Inferences from fungi on the evolution of anisogamy and mating types. Biol Rev Camb Philos Soc 86:421–442. <https://doi.org/10.1111/j.1469-185X.2010.00153.x>.
  47. Yun SH, Berbee ML, Yoder OC, Turgeon BG. 1999. Evolution of the fungal self-fertile reproductive life style from self-sterile ancestors. Proc Natl Acad Sci U S A 96:5592–5597. <https://doi.org/10.1073/pnas.96.10.5592>.
  48. Schurko AM, Neiman M, Logsdon JM. 2009. Signs of sex: what we know and how we know it. Trends Ecol Evol 24:208–217. <https://doi.org/10.1016/j.tree.2008.11.010>.
  49. de Man TJB, Stajich JE, Kubicek CP, Teiling C, Chenthamara K, Atanasova L, Druzhinina IS, Levenkova N, Birnbaum SSL, Barribeau SM, Bozick BA, Suen G, Currie CR, Gerardo NM. 2016. Small genome of the fungus *Escovopsis weberi*, a specialized disease agent of ant agriculture. Proc Natl Acad Sci U S A 113:3567–3572. <https://doi.org/10.1073/pnas.1518501113>.
  50. Ohsawa T, Saito Y, Sawada H, Ide Y. 2008. Impact of altitude and topography on the genetic diversity of *Quercus serrata* populations in the Chichibu Mountains, central Japan. Flora 203:187–196. <https://doi.org/10.1016/j.flora.2007.02.007>.
  51. Burdon JJ, Thrall PH, Ericson L. 2013. Genes, communities and invasive species: understanding the ecological and evolutionary dynamics of host-pathogen interactions. Curr Opin Plant Biol 16:400–405. <https://doi.org/10.1016/j.pbi.2013.05.003>.
  52. Zhan J, Thrall PH, Burdon JJ. 2014. Achieving sustainable plant disease management through evolutionary principles. Trends Plant Sci 19: 570–575. <https://doi.org/10.1016/j.tplants.2014.04.010>.
  53. Praz CR, Bourras S, Zeng F, Sánchez-Martín J, Menardo F, Xue M, Yang L, Roffler S, Böni R, Herren G, McNally KE, Ben-David R, Parlange F, Oberhaensli S, Flückiger S, Schäfer LK, Wicker T, Yu D, Keller B. 2017. *AvrPm2* encodes an RNase-like avirulence effector which is conserved in the two different specialized forms of wheat and rye powdery mildew fungus. New Phytol 213:1301–1314. <https://doi.org/10.1111/nph.14372>.
  54. Kusch S, Frantzeskakis L, Thieron H, Panstruga R. 2018. Small RNAs from cereal powdery mildew pathogens may target host plant genes. Fungal Biol 122:1050–1063. <https://doi.org/10.1016/j.funbio.2018.08.008>.
  55. Pennington HG, Gheorghe DM, Damerum A, Pliego C, Spanu PD, Cramer R, Bindschedler LV. 2016. Interactions between the powdery mildew effector BEC1054 and barley proteins identify candidate host



- targets. *J Proteome Res* 15:826–839. <https://doi.org/10.1021/acs.jproteome.5b00732>.
56. Saur JM, Bauer S, Kracher B, Lu X, Franzeskakis L, Müller MC, Sabelleck B, Kümmel F, Panstruga R, Maekawa T, Schulze-Lefert P. 2019. Multiple pairs of allelic MLA immune receptor-powdery mildew AVR<sub>A</sub> effectors argue for a direct recognition mechanism. *eLife* 8:e44471. <https://doi.org/10.7554/eLife.44471>.
  57. Spanu PD, Pennington HG, Jones R, Kwon S, Bonciani G, Thieron H, Chandler T, Luong P, Morgan S, Przydacz M, Bozkurt TO, Bowden S, Craze M, Wallington E, Garnett J, Kwaitaal M, Panstruga R, Cota E. 2018. A fungal ribonuclease-like effector protein inhibits plant host ribosomal RNA degradation. *bioRxiv* <https://doi.org/10.1101/291427>.
  58. Delulio GA, Guo L, Zhang Y, Goldberg JM, Kistler HC, Ma L-J. 2018. Kinome expansion in the *Fusarium oxysporum* species complex driven by accessory chromosomes. *mSphere* 3:e00231-18. <https://doi.org/10.1128/mSphere.00231-18>.
  59. Meyer F, Bagchi S, Chaterji S, Gerlach W, Grama A, Harrison T, Paczian T, Trimble WL, Wilke A. 2017. MG-RAST version 4—lessons learned from a decade of low-budget ultra-high-throughput metagenome analysis. *Brief Bioinform* <https://doi.org/10.1093/bib/bbx105>.
  60. Jiang H, Lei R, Ding S-W, Zhu S. 2014. Skewer: a fast and accurate adapter trimmer for next-generation sequencing paired-end reads. *BMC Bioinformatics* 15:182. <https://doi.org/10.1186/1471-2105-15-182>.
  61. Li H. 2015. BFC: correcting Illumina sequencing errors. *Bioinformatics* 31:2885–2887. <https://doi.org/10.1093/bioinformatics/btv290>.
  62. Bankevich A, Nurk S, Antipov D, Gurevich AA, Dvorkin M, Kulikov AS, Lesin VM, Nikolenko SI, Pham S, Prjibelski AD, Pyshkin AV, Sirotkin AV, Vyahhi N, Tesler G, Alekseyev MA, Pevzner PA. 2012. SPAdes: a new genome assembly algorithm and its applications to single-cell sequencing. *J Comput Biol* 19:455–477. <https://doi.org/10.1089/cmb.2012.0021>.
  63. Levy A, Salas Gonzalez I, Mittelviehhaus M, Clingenpeel S, Herrera Paredes S, Miao J, Wang K, Devescovi G, Stillman K, Monteiro F, Rangel Alvarez B, Lundberg DS, Lu T-Y, Lebeis S, Jin Z, McDonald M, Klein AP, Feltcher ME, Rio TG, Grant SR, Doty SL, Ley RE, Zhao B, Venturi V, Pelletier DA, Vorholt JA, Tringe SG, Woyke T, Dangl JL. 2018. Genomic features of bacterial adaptation to plants. *Nat Genet* 50:138–150. <https://doi.org/10.1038/s41588-017-0012-9>.
  64. Camacho C, Coulouris G, Avagyan V, Ma N, Papadopoulos J, Bealer K, Madden TL. 2009. BLAST+: architecture and applications. *BMC Bioinformatics* 10:421. <https://doi.org/10.1186/1471-2105-10-421>.
  65. Holt C, Yandell M. 2011. MAKER2: an annotation pipeline and genome-database management tool for second-generation genome projects. *BMC Bioinformatics* 12:491. <https://doi.org/10.1186/1471-2105-12-491>.
  66. Jones P, Binns D, Chang H-Y, Fraser M, Li W, McAnulla C, McWilliam H, Maslen J, Mitchell A, Nuka G, Pesseat S, Quinlan AF, Sangrador-Vegas A, Scheremetjew M, Yong S-Y, Lopez R, Hunter S. 2014. InterProScan 5: genome-scale protein function classification. *Bioinformatics* 30:1236–1240. <https://doi.org/10.1093/bioinformatics/btu031>.
  67. Finn RD, Clements J, Eddy SR. 2011. HMMER web server: interactive sequence similarity searching. *Nucleic Acids Res* 39:W29–W37. <https://doi.org/10.1093/nar/gkr367>.
  68. Huang L, Zhang H, Wu P, Entwistle S, Li X, Yohe T, Yi H, Yang Z, Yin Y. 2018. dbCAN-seq: a database of carbohydrate-active enzyme (CAZyme) sequence and annotation. *Nucleic Acids Res* 46:D516–D521. <https://doi.org/10.1093/nar/gkx894>.
  69. Petersen TN, Brunak S, von Heijne G, Nielsen H. 2011. SignalP 4.0: discriminating signal peptides from transmembrane regions. *Nat Methods* 8:785–786. <https://doi.org/10.1038/nmeth.1701>.
  70. Emanuelsson O, Brunak S, von Heijne G, Nielsen H. 2007. Locating proteins in the cell using TargetP, SignalP and related tools. *Nat Protoc* 2:953–971. <https://doi.org/10.1038/nprot.2007.131>.
  71. Testa AC, Oliver RP, Hane JK. 2016. OcculterCut: a comprehensive survey of AT-rich regions in fungal genomes. *Genome Biol Evol* 8:2044–2064. <https://doi.org/10.1093/gbe/evw121>.
  72. Hane JK, Oliver RP. 2008. RIPCAL: a tool for alignment-based analysis of repeat-induced point mutations in fungal genomic sequences. *BMC Bioinformatics* 9:478. <https://doi.org/10.1186/1471-2105-9-478>.
  73. Emms DM, Kelly S. 2015. OrthoFinder: solving fundamental biases in whole genome comparisons dramatically improves orthogroup inference accuracy. *Genome Biol* 16:157. <https://doi.org/10.1186/s13059-015-0721-2>.
  74. Price MN, Dehal PS, Arkin AP. 2010. FastTree 2—approximately maximum-likelihood trees for large alignments. *PLoS One* 5:e9490. <https://doi.org/10.1371/journal.pone.0009490>.
  75. Katoh K, Standley DM. 2013. MAFFT multiple sequence alignment software version 7: improvements in performance and usability. *Mol Biol Evol* 30:772–780. <https://doi.org/10.1093/molbev/mst010>.
  76. Letunic I, Bork P. 2016. Interactive tree of life (iTOL) v3: an online tool for the display and annotation of phylogenetic and other trees. *Nucleic Acids Res* 44:W242–W245. <https://doi.org/10.1093/nar/gkw290>.
  77. Li H. 2013. Aligning sequence reads, clone sequences and assembly contigs with BWA-MEM. *arXiv* <https://arxiv.org/abs/1303.3997>. Accessed 28 October 2017.
  78. Li H, Handsaker B, Wysoker A, Fennell T, Ruan J, Homer N, Marth G, Abecasis G, Durbin R. 2009. The Sequence Alignment/Map format and SAMtools. *Bioinformatics* 25:2078–2079. <https://doi.org/10.1093/bioinformatics/btp352>.
  79. Cingolani P, Patel VM, Coon M, Nguyen T, Land SJ, Ruden DM, Lu X. 2012. Using *Drosophila melanogaster* as a model for genotoxic chemical mutational studies with a new program, SnpSift. *Front Genet* 3:35. <https://doi.org/10.3389/fgene.2012.00035>.